Histol Histopathol (2015) 30: 987-999

http://www.hh.um.es

Histology and Histopathology

Cellular and Molecular Biology

N-Cadherin, ADAM-10 and Aquaporin 1 expression in lung tissue exposed to fluoro-edenite fibers: an immunohistochemical study

Giuseppe Musumeci[1]*, Carla Loreto[1]*, Marta Anna Szychlinska[1], Rosa Imbesi[1], Venerando Rapisarda[2], Flavia Concetta Aiello[1], Sergio Castorina[1] and Paola Castrogiovanni[1]

[1]Department of Biomedical Sciences and Biotechnologies, Human Anatomy and Histology Section, School of Medicine and [2]Division of Occupational Medicine, University Hospital "Policlinico- Vittorio Emanuele", University of Catania, Catania, Italy

*Joint first authors

Summary. Fluoro-edenite (FE) fibers are similar to other amphibole asbestos fibers. The scientific relevance of FE is due to its ability to lead to chronic inflammation and carcinogenesis in lung tissue shown after its inhalation. These fibers stimulate aberrant host cell proliferation and induce the release of cytokines, growth factors, reactive oxygen and nitrite species, which results in DNA damage. In previous studies, we showed that FE induces functional modifications in sheep and human lung fibroblasts and alveolar epithelial cells, where the overexpression of several molecules probably involved in pathological cellular mechanisms induced by FE exposition have been detected. However, the mechanisms of cellular and molecular toxicity and the cellular response to FE fibers are still not well known. N-cadherin, ADAM-10 and AQP1 are molecules involved in carcinogenesis and in inflammatory process. In this study we analyzed, through immunohistochemistry, their expression in the lung tissue of sheep exposed to FE. Our results showed different patterns of immunolabeling for N-cadherin, ADAM-10 and AQP1. N-cadherin and ADAM-10 were more expressed in FE exposed lung tissue, when compared with the control. On the contrary, AQP1 was more expressed in non exposed lung tissue. These results suggest that N-Cadherin, ADAM-10 and AQP1 are probably involved in different pathological processes induced by FE fiber exposition. The aim of the study was to better understand the mechanisms of cellular and molecular toxicity and of cellular response to FE fibers in order to identify, in the future, a possible therapeutic intervention in cases of FE-associated pathogenesis.

Key words: Fluoro-edenite fibers, N-cadherin, ADAM-10, AQP1, lung tissue

Offprint requests to: Dr. Giuseppe. Musumeci, Ph.D, Department of Biomedical Sciences and Biotechnologies, Human Anatomy and Histology Section, School of Medicine, University of Catania, 95123 Catania, Italy. e-mail: g.musumeci@unict.it.

DOI: 10.14670/HH-11-603

Introduction

Fluoro-edenite ($NaCa_2Mg_5Si_7AlO_{22}F$) (FE) is a new mineral species, identified by the Commission on New Minerals and Mineral Names (CNMMN) of the International Mineralogical Association (IMA) as a new amphibole end-member (Gianfagna and Oberti, 2001). FE fibers are similar to other amphibole asbestos fibers (Comba et al., 2003) found in mountain and volcanic areas in Italy and other parts of the world where they, probably, are a cause of the increased incidence of lung cancer and other lung diseases (Cardile et al., 2007). FE fibers are typical of benmoreitic lavas and they are used as the materials for buildings and road pavements (Comba et al., 2003; Biggeri et al., 2004; Musumeci et al., 2011) in Biancavilla, a town of eastern Sicily (Italy), where the epidemiological studies highlighted a cluster of mortality from pleural mesothelioma (Paoletti et al., 2000) and established the role of these fibers in causing chronic obstructive lung disease (Biggeri et al., 2004). The scientific relevance of FE depends on the fact that

inhalation of FE fibers can cause chronic inflammation and carcinogenesis in lung tissue (Paoletti et al., 2000; Rinaudo et al., 2006). In fact, FE fibers can stimulate host cell proliferation and the release of cytokines, growth factors, reactive oxygen species (ROS) and reactive nitrogen species (RNS), which results in DNA damage (Kamp and Weitzman, 1999; Szychlinska et al., 2014). In previous studies, we showed that FE induces functional modifications in sheep and human lung fibroblasts and alveolar epithelial cells, resulting in consequent DNA damage (Martinez et al., 2006; Loreto et al., 2009), while in an *in vivo* lung model, it activates the apoptosis mechanisms and modifies the expression of retinoblastoma (Rb) proteins (Loreto et al., 2008; Musumeci et al., 2010, 2011). However, the mechanisms of cellular and molecular toxicity and the cellular response to FE fibers are still not well known (Musumeci et al., 2011). N-cadherin (N-Cad) is a cell-cell junction protein (135-kDa) found in nerve cells (Redies et al., 1993), developing muscle cells (Soler and Knudsen, 1994) and mesothelial cells (Hatta et al., 1987). The literature reports that N-Cad is overexpressed in lung cancer and particularly in malignant pleural mesothelioma (Abutaily et al., 2003; Nelson and Ordonez, 2003; King et al., 2006). Authors showed that in bladder cancer, the increased expression of N-Cad testifies the epithelial-mesenchymal transition (EMT), which represents the initial stage of metastatic progression. The latter is induced by the downregulation of homeodomain-interacting protein kinase-2 (Hipk2), a serine/threonine kinase involved in tumor suppression (Cai et al., 2013; Tan et al., 2014; Musumeci et al., 2014a). ADAM-10 (a "disintegrin and metalloprotease") is an ADAMs family member that mediates ectodomain shedding of integral membrane proteins. It is essential for a number of developmental and physiological processes (Tousseyn et al., 2006; Reiss and Saftig, 2009). Dysregulation of ADAM-10-mediated ectodomain shedding is associated with several diseases (Saftig and Reiss, 2011) and its overexpression has been reported in various types of cancer (Wu et al., 1997; Yoshimura et al., 2002; Fogel et al., 2003; McCulloch et al., 2004; Gavert et al., 2005; Murphy, 2008), suggesting its direct role in tumor progression (Saftig and Reiss, 2011). ADAM-10 is also able to modulate inflammatory responses through several pathways (Matthews et al., 2003; Hundhausen et al., 2007; Schulz et al., 2008; Hikita et al., 2009). Aquaporin 1 (AQP1) is a member of aquaporins (AQPs), hydrophobic membrane channel proteins, which mediate the selective crossing of water molecules through biological membranes, influencing the osmotic homeostasis of cells (Mobasheri and Marples, 2004; Wang and Zhu, 2011). AQP expression was widely studied in respiratory tract, kidney, gastrointestinal tract, brain, eye, and other tissues (Liang et al., 2008; Sindelar et al., 2000; Loreto et al., 2012; Musumeci et al., 2013a). It has been demonstrated that AQPs play a relevant role in cell volume control, active near-isosmolar fluid absorption/secretion, neuronal signal transduction, tumor angiogenesis and cell metabolism, proliferation and migration (Verkman, 2009). N-Cad, ADAM-10 and AQP1 seem to be actively involved in carcinogenesis and in the inflammatory process. Hence, our interest is to study their expression in the lung tissue of sheep exposed to FE, in order to confirm the toxic effect of its accidentally inhaled fibers, already reported in our previous articles (Martinez et al., 2006; Loreto et al., 2008, 2009; Musumeci et al., 2010, 2011). In particular, we considered it interesting to analyze N-Cad and its possible involvement in the onset of cancer, such as the pleural mesothelioma; the selection of ADAM-10 was due to its possible role both in the inflammatory processes related to exposure to the FE fibers and in the eventual onset of carcinogenesis; the selection of AQP1 had a completely different meaning, in fact AQP1 has an important regulatory role for cell volume and extracellular matrix homeostasis, and in the present study we wanted to analyze its possible involvement in the endogenous regulatory mechanisms activated by FE fiber exposure in order to restore tissue homeostasis. The aim of this study was to better understand the mechanisms of cellular and molecular toxicity and of cellular response to FE fibers in order to identify, in the future, a possible therapeutic intervention in cases of FE-associated pathogenesis.

Material and methods

Animals

Sixty sheep of both sexes (n=60), randomly selected from six exposed flocks (n=360) habitually grazing 3 km from the town of Biancavilla, and ten control sheep (n=10), from a flock (n=60) habitually grazing about 50 km from the Biancavilla stone quarry, were sacrificed in a slaughterhouse and used for this study. Ante- and post-mortem examinations were conducted by a veterinary surgeon to establish the state of health of each sheep (according to Community Regulation CE n. 854/04 and council of 29 April 2004). The age range of exposed and control animals was 4.0-6.5 years.

Histology

Lung tissue (1 cm^3) from the right apical lobe and the principal and accessory lung lobes were rinsed in phosphate buffered saline (PBS), fixed in 10% buffered-formalin as previously described (Martinez et al., 2006; Loreto et al., 2008). After an overnight wash, specimens were dehydrated in graded ethanol, cleared in xylene and paraffin-embedded, preserving their anatomical orientation. Sections (4-5 μm in thickness) were cut from paraffin blocks using a microtome, mounted on sialinate-coated slides and stored at room temperature. The sections were then stained with hematoxylin and eosin (H&E) and examined using a Zeiss Axioplan light

microscope (Carl Zeiss, Oberkochen, Germany) for general morphological characterization and to highlight the presence or absence of structural alterations. Finally, representative photomicrographs were captured using a digital camera (AxioCam MRc5, Carl Zeiss, Oberkochen, Germany).

Immunohistochemistry (IHC)

Lung tissue (1 cm^3), from the right apical lobe and the principal and accessory lung lobes, was collected from each subject and fixed in 10% buffered formalin for 2 h; after an overnight wash, specimens were dehydrated in graded ethanol and paraffin-embedded. Sections 3-4 μm in thickness were cut, mounted on silane-coated slides (Dako, Glostrup, Denmark), and air-dried. For immunohistochemical analysis, specimens were processed as previously described (Loreto et al., 2013). Briefly, the slides were dewaxed in xylene, hydrated using graded ethanols and were incubated for 30 min in 0.3% H_2O_2/methanol solution to quench endogenous peroxidase activity and then rinsed for 20 min with phosphate-buffered saline (PBS; Sigma, Milan, Italy). The sections were heated (5 min x 3) in capped polypropylene slide-holders with citrate buffer (10 mM citric acid, 0.05% Tween 20, pH 6.0; Bio-Optica, Milan, Italy), using a microwave oven (750 W) to unmask antigenic sites. The blocking step was performed before application of the primary antibody with 5% bovine serum albumin (BSA; Sigma, Milan, Italy) in PBS for 1 hour in a humid chamber. BSA was used as a blocking agent to prevent non-specific binding of the primary and secondary antibodies to the tissue sections. Following blocking, the sections were incubated overnight at 4°C with mouse monoclonal Anti-N-Cad antibody clone 13A9 (05-915; EMD Millipore Corporation, Billerica, MA, USA), diluted 1:400 in phosphate buffer saline (PBS; Sigma, Milan, Italy); rabbit polyclonal Anti-ADAM-10 antibody (ab1997; abcam, Cambridge, UK), diluted 1:200 in phosphate buffer saline (PBS; Sigma, Milan, Italy); mouse monoclonal Anti-AQP1 antibody (Santa Cruz Biotechnology, Inc., USA) diluted 1:100 in phosphate buffer saline (PBS; Sigma, Milan, Italy). Immune complexes were then treated with a biotinylated link antibody and then detected with peroxidase labeled streptavin, both incubated for 10 min at room temperature (LSAB+ System-HRP, K0690; Dako, Glostrup, Denmark). The immunoreaction was visualized by incubating the sections for 2 minutes in a 0.1% 3,3'-diaminobenzidine and 0.02% hydrogen peroxide solution (DAB substrate Chromogen System; Dako, Denmark). The sections were lightly counterstained with Mayer's hematoxylin (Histolab Products AB, Göteborg, Sweden) mounted in GVA (Zymed Laboratories, San Francisco, CA, USA) and observed with an Axioplan Zeiss light microscope (Carl Zeiss, Oberkochen, Germany) and photographed with a digital camera (AxioCam MRc5, Carl Zeiss, Oberkochen, Germany)

Evaluation of immunohistochemistry (IHC)

The antibodies-staining (N-Cad, ADAM-10 and AQP1) status was identified as either negative or positive. Immunohistochemical positive staining was defined by the presence of brown chromogen detection on the edge of the hematoxylin-stained cell nucleus, distributed within the cytoplasm or in the membrane via evaluation by light microscopy as previously described (Musumeci et al., 2013b). Positive and negative controls were performed to test the specific reaction of primary antibodies used in this study at a protein level. Positive controls consisted of tissue specimens with known antigenic positivity. Sections treated with PBS without the primary antibodies served as negative controls. Seven fields, randomly selected from each section, were analyzed for morphometric and densitometric analysis. The percentage areas (morphometric analysis) stained with antibodies (N-Cad, ADAM-10 and AQP1), expressed as % positive, dark brown pixels of the analyzed fields, and the level (high/low) of staining intensity of positive areas (densitometric analysis), expressed as densitometric count ($pixel^2$) of positive, dark brown pixels of the analyzed fields, were calculated using software for image acquisition (AxioVision Release 4.8.2 - SP2 Software, Carl Zeiss Microscopy GmbH, Jena, Germany), (Musumeci et al., 2013c). Data were expressed as mean±standard deviation (SD). Statistical significance of results was thus accomplished. Digital micrographs were taken using the Zeiss Axioplan light microscope (Carl Zeiss, Oberkochen, Germany) fitted with a digital camera (AxioCam MRc5, Carl Zeiss,

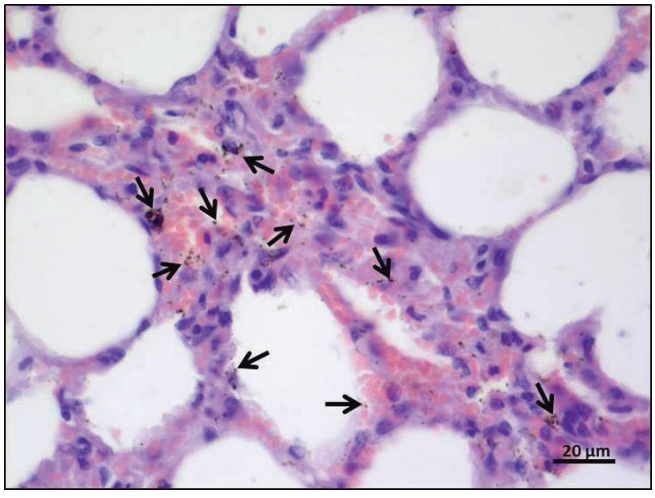

Fig. 1. Haematoxylin & Eosin staining. Fluoro-edenite fibres (black arrows) in close contact with lung alveolar epithelium and interstitium. Scale bar: 20 μm.

Oberkochen, Germany); evaluations were made by three blinded investigators, whose evaluations were assumed to be correct if values were not significantly different. In case of dispute concerning interpretation, the case was reconsidered to reach an unanimous agreement as previously described (Musumeci et al., 2013d).

Statistical analysis

Statistical analysis was performed using SPSS software (SPSS® release 16.0, Chicago, IL, USA). Data were tested for normality with the Kolmogorov-Smirnov test. All variables were normally distributed. Comparisons between two means were tested with the unpaired t-test with Welch correction. P-values of less than 0.05 were considered statistically significant. Data are presented as the mean±SD. Cohen's kappa was applied to measure the agreement between the three observers and averaged to evaluate overall agreement as previously described (Musumeci et al., 2014b).

Results

Histology

We performed histopathological analysis with Hematoxylin & Eosin that confirmed the presence of FE fibers in the lung tissue of exposed sheep (Fig. 1) as already reported in our previous studies (Martinez et al., 2006; Loreto et al., 2008).

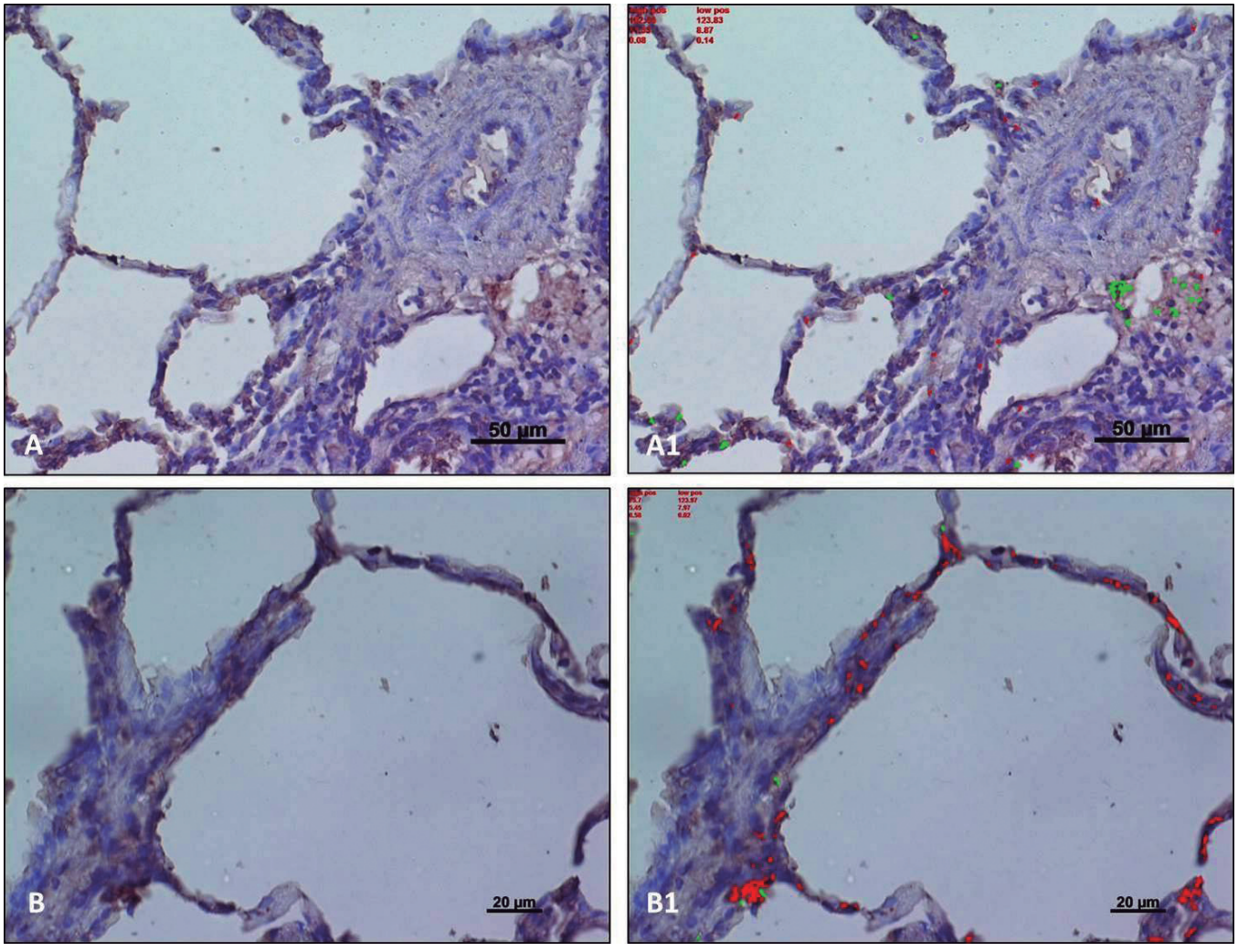

Fig. 2. N-cadherin immunostaining in lung tissue of non exposed sheep. **A-A1.** Section of lung tissue with alveoli and bronchial tubes, and its image analysis by software in which only traces of N-cad immunostaining were detected (green and red color). **B-B1.** Section of lung tissue with alveoli, and its image analysis by software in which very low N-cad immunostaining was detected (red color). Scale bar: A, A1, 50 μm; B, B1, 20 μm.

Immunohistochemistry (IHC)

In the present study, we evaluated the expression of N-Cad, ADAM-10 and AQP1 in lung tissue of sheep exposed to FE fibers.

Densiometric analysis

Densitometric count (pixel^2) of stained areas by N-Cad, ADAM-10 and AQP1, expressed by dark brown pixels of the analyzed fields, was considered as described below:

N-Cad

In lung tissue of non exposed sheep, insignificant traces of N-Cad immunostaining were detected (Figs. 2A,A1, 2B,B1). In exposed sheep lung, a high (red color) expression of N-Cad was detected in interstitial areas of reactive fibrosis (consequence of FE fibers exposition) and a low (green color) N-Cad immunolabeling was also detected but to a lesser degree (Fig. 3A,A1). High expression of N-Cad was also demonstrated in the alveolar epithelium and interstitium between alveoli and a low (green color) N-Cad immunostaining was also detected but to a lesser degree (Fig. 3B,B1). Statistical analysis showed that the difference between N-Cad expression in exposed lung tissue vs. non exposed lung tissue was statistically significant ($p<0.05$), both in interstitium and alveoli (Fig. 4).

ADAM-10

In lung tissue of non exposed sheep, no ADAM-10 immunolabeling was detected (Fig. 5A,A1,B,B1). In

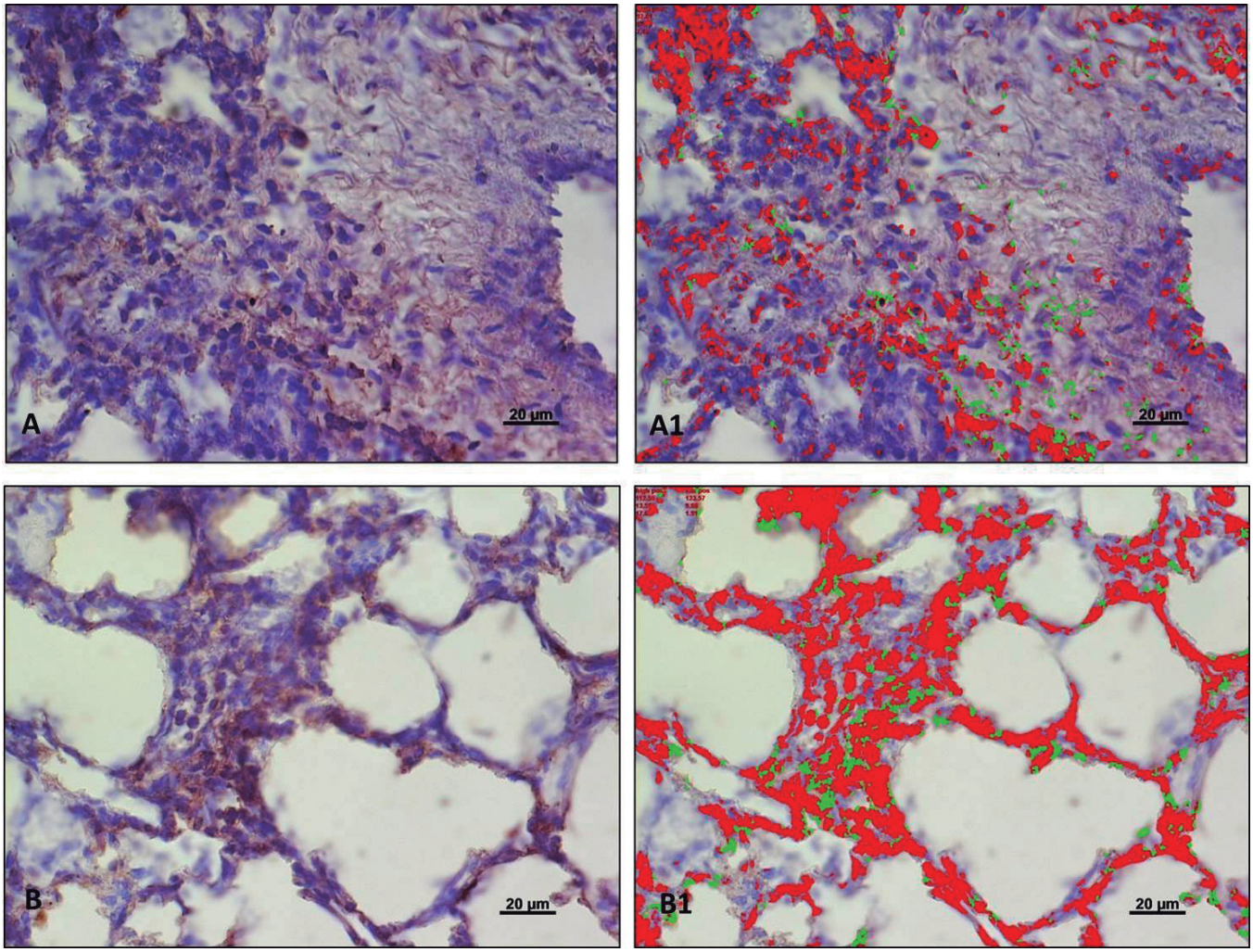

Fig. 3. N-cadherin immunostaining in lung tissue of exposed sheep. **A-A1.** Section of lung tissue with interstitium in an area of reactive fibrosis, and its image analysis by software in which mostly high immunostaining (red color) mixed with low immunostaining (green color) were detected. **B-B1.** Section of lung tissue with alveoli and intraparenchymal stroma, and its image analysis by software in which mostly high immunostaining (red color) mixed with low immunostaining (green color) were detected. Scale bar: 20 μm.

exposed sheep lung, a low (green color) expression of ADAM-10 was detected in the intraparenchymal stroma around bronchioles, in bronchiolar epithelium and in the alveolar epithelium (Fig. 6A,A1). A high (red color) ADAM-10 immunolabeling was also detected but to a lesser degree (Fig. 6B,B1). Statistical analysis showed that the difference between ADAM-10 expression in exposed lung tissue vs. non exposed lung tissue was statistically significant both in bronchioles and alveoli ($p<0.05$) (Fig. 7).

AQP1

Finally, in lung tissue of non exposed sheep, a low (green color) AQP1 immunostaining was detected in the intraparenchymal stroma around bronchial tubes, in bronchial epithelium, in interlobular septa and in the alveolar epithelium (Fig. 8A,A1,B,B1). In exposed

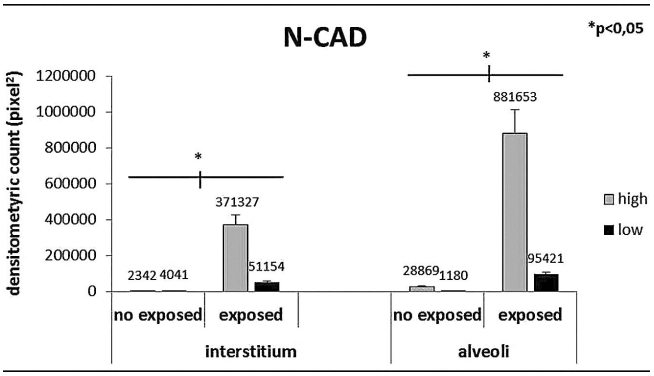

Fig. 4. Graph. A bar chart representing a comparison of the immunostaining intensity in N-cad positive areas of non exposed sheep (n. 10) vs. exposed sheep (n. 60), expressed by densitometric count (pixel2) of dark brown pixels of the analyzed fields. Gray bars, high immunostaining; black bars, low immunostaining. Data are presented as mean±SD. *p<0,05.

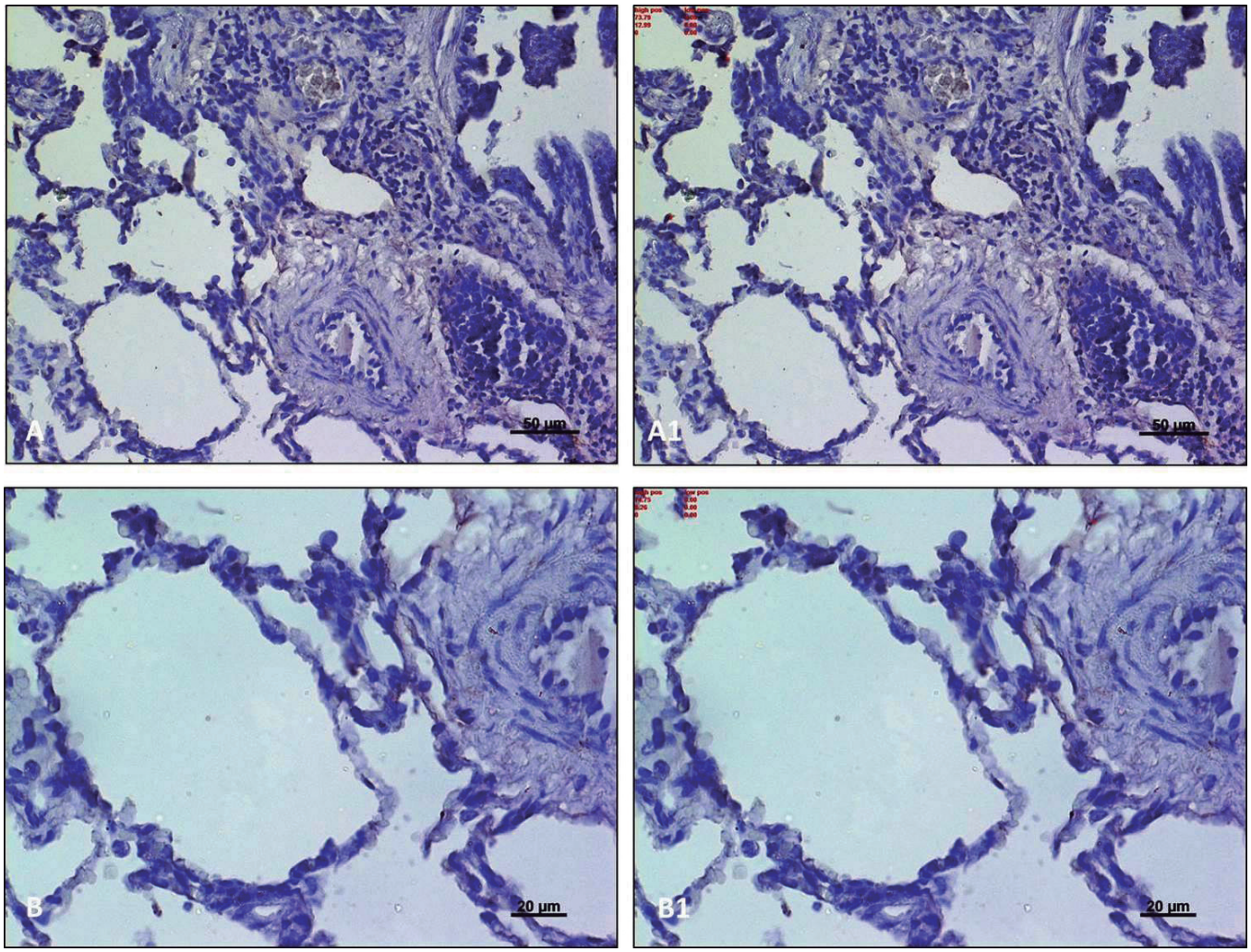

Fig. 5. ADAM-10 immunostaining in lung tissue of non exposed sheep. **A-A1.** Section of lung tissue with alveoli, bronchial tubes and intraparenchymal stroma, and its image analysis by software in which no immunolabeling was detected. **B-B1.** Section of lung tissue with alveoli, and its image analysis by software in which no immunolabeling was detected. Scale bar: A, A1, 50 μm; B, B1, 20 μm.

sheep lung, a high (red color) mixed to a low (green color) expression of AQP1 was detected in fibrotic interstitium around bronchial tubes and in some areas of bronchial epithelium (Fig. 9A,A1). No AQP1 immunostaining was detected in interstitium between alveoli and in alveolar epithelium (Fig. 9B,B1). Statistical analysis showed that the difference between the total (high + low) AQP1 expression in bronchial tubes of exposed sheep vs. non exposed ones was statistically significant ($p<0.05$) (Fig. 10). Instead, in alveolar epithelium AQP1 immunolabeling is present only in non exposed lung tissue, and so the difference between AQP1 expression in exposed sheep vs. non exposed ones remains again statistically significant ($p<0.05$), but inversely with respect to bronchial tubes (Fig. 10).

Morphometric analysis

The % of stained areas by N-Cad, ADAM-10 and AQP1, expressed by dark brown pixels of the analyzed fields, were considered. From analysis of immunolabeling extension, the percentage of immunostained areas by N-Cad and ADAM-10 was much higher in exposed sheep compared with non exposed ones ($p<0.05$). On the contrary, although distribution and intensity of AQP1 immunolabeling showed a more complex pattern as reported above, the total percentage of immunostained areas by AQP1 was higher in non exposed sheep compared to the exposed

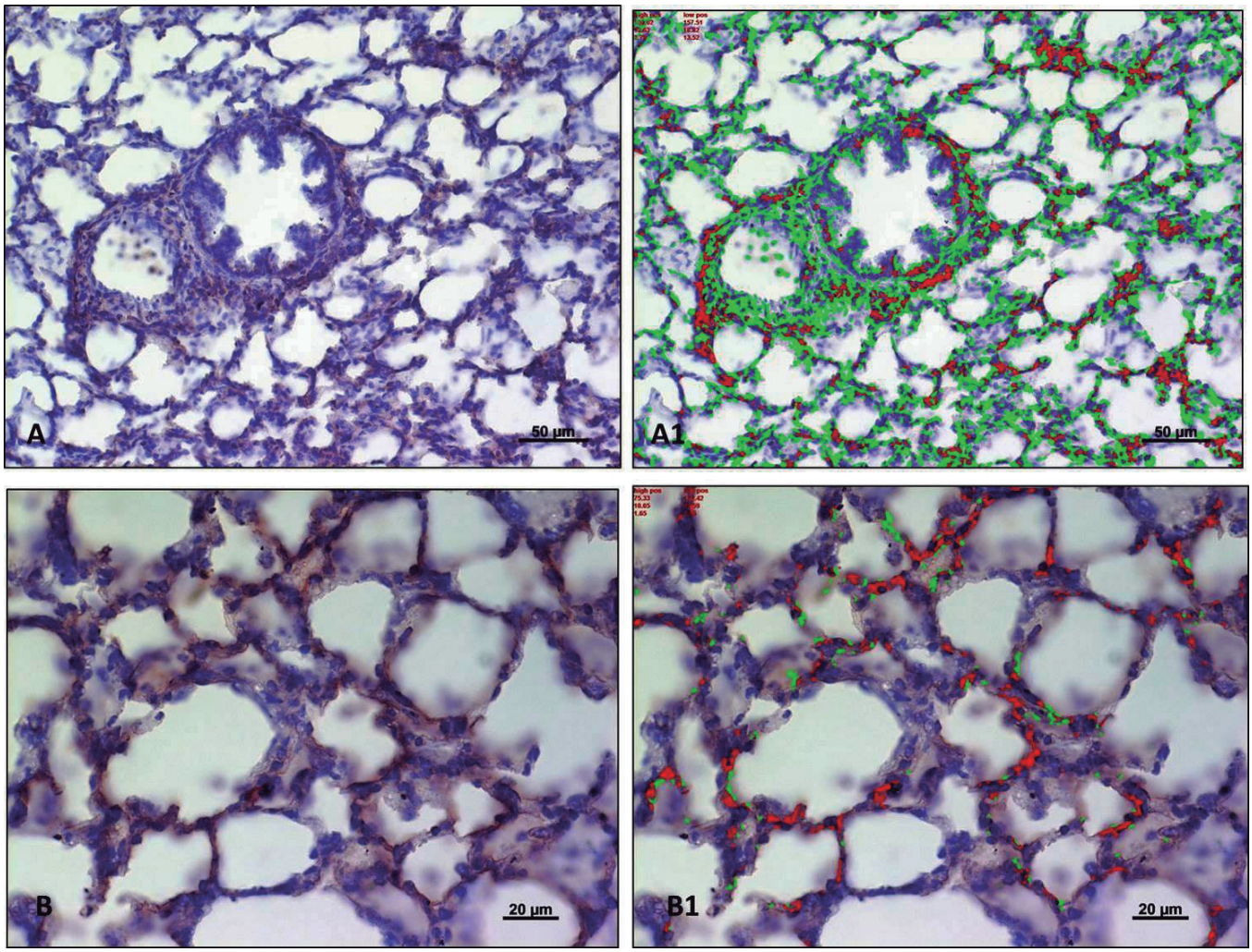

Fig. 6. ADAM-10 immunostaining in lung tissue of exposed sheep. **A-A1.** Section of lung tissue with alveoli, bronchioles and bronchial tubes, and its image analysis by software in which mostly low immunostaining (green color) mixed with high immunostaining (red color) were detected. **B-B1.** Section of lung tissue with alveoli, and its image analysis by software in which mostly high immunostaining (red color) mixed with low immunostaining (green color) were detected. Scale bar: A, A1, 50 μm; B, B1, 20 μm.

ones ($p<0.05$) e (Fig. 11).

Discussion

FE fibers, similar to other asbestos fibers (Comba et al., 2003), are typical of volcanic areas such as Biancavilla, where epidemiological studies showed their

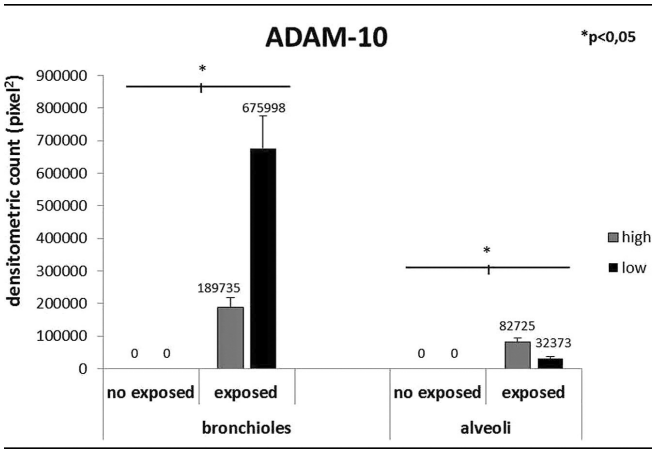

Fig. 7. Graph. A bar chart representing a comparison of the immunostaining intensity in ADAM-10 positive areas of non exposed sheep (n. 10) vs. exposed sheep (n. 60), expressed by densitometric count (pixel^2) of dark brown pixels of the analyzed fields. Gray bars, high immunostaining; black bars, low immunostaining. Data are presented as mean±SD. *p<0,05.

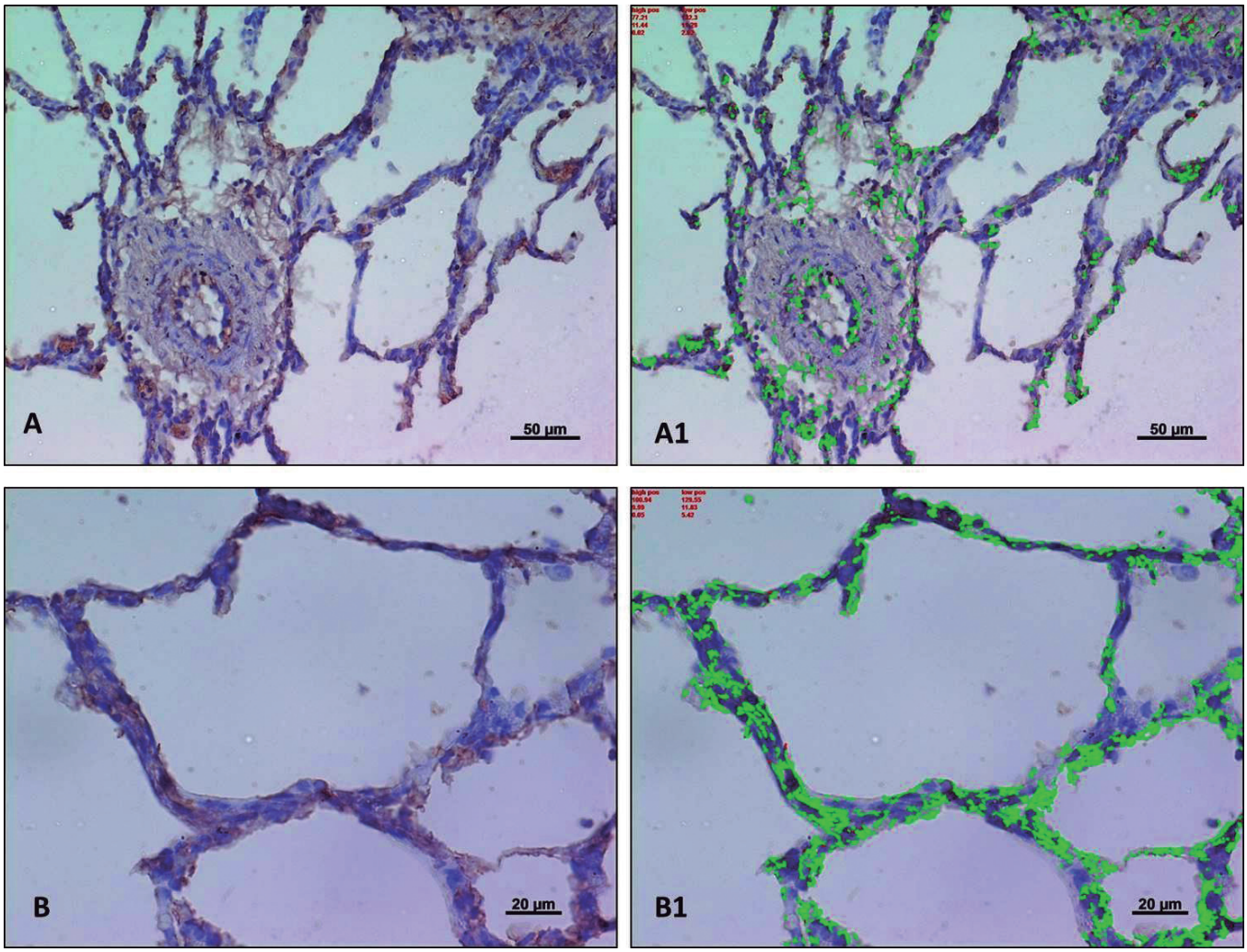

Fig. 8. AQP1 immunostaining in lung tissue of non exposed sheep. **A-A1.** Section of lung tissue with alveoli, bronchial tubes and intraparenchymal stroma, and its image analysis by software in which low immunostaining (green color) was detected. **B-B1.** Section of lung tissue with alveoli, and its image analysis by software in which low immunostaining (green color) was detected. Scale bar: A, A1, 50 μm; B, B1, 20 μm.

involvement in pleural mesothelioma and chronic lung disease (Paoletti et al., 2000; Biggeri et al., 2004; Cardile et al., 2007). Different insights exist about the reaction of the lung cells to the exposure to FE fibers (Szychlinska et al., 2014). Prolonged inhalation of FE fibers can cause chronic inflammation and carcinogenesis in lung tissue (Paoletti et al., 2000; Rinaudo et al., 2006) due to their capacity to stimulate the aberrant host cell proliferation and to induce the release of cytokines, growth factors ROS and RNS, which are responsible for DNA damage (Kamp et al., 1992; Kamp and Weitzman, 1999; Szychlinska et al., 2014). Recent data from the literature suggest that oxidative stress may play a critical role in malignant pleural mesothelioma carcinogenesis, promoting an EMT and enhancing the expression of stemness genes (Kim et al., 2013; Szychlinska et al., 2014). Moreover, it was described that FE fibers induce aberrant cell motility, distribution of polymerized actin and ß-catenin expression, underlying their involvement in cancer pathogenesis (Pugnaloni et al., 2007). Authors reported that the sheep lung is comparable to the human one (Begin et al., 1981), therefore the sheep model of asbestosis is an appropriate tool to study the pathophysiology of lung disease (Lee et al., 1997). In our previous studies we confirmed the inflammatory pathophysiology of FE fibers in lung tissue and their possible involvement in carcinogenesis. We observed the overexpression of matrix metalloproteinase protein 13 (MMP-13) associated with fibrosis and of TNF-related apoptosis inducing ligand (TRAIL) and its death receptor 5 (DR5), confirming the link between FE fiber

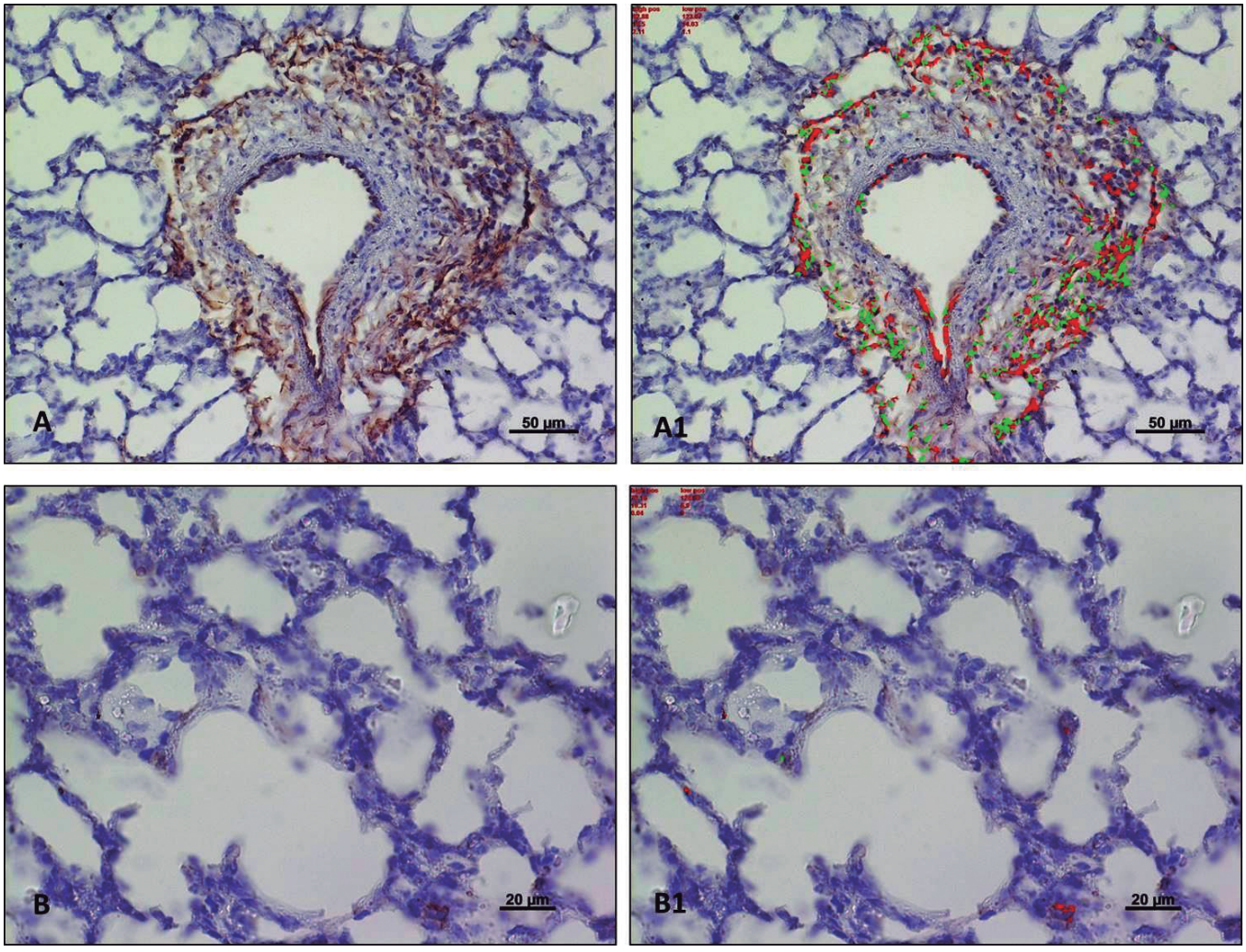

Fig. 9. AQP1 immunostaining in lung tissue of exposed sheep. **A-A1.** Section of lung tissue with alveoli, bronchial tubes and intraparenchymal stroma, and its image analysis by software in which mostly high immunostaining (red color) mixed with low immunostaining (green color) were detected. **B-B1.** Section of lung tissue with alveoli, and its image analysis by software in which no immunostaining was detected. Scale bar: A, A1, 50 μm; B, B1, 20 μm.

exposure and epithelial cell apoptosis at site of the initial fiber deposition (Martinez et al., 2006). Moreover, a low bcl-2 (anti-apoptotic protein) immunoreactivity and bax (pro-apoptotic protein) up-regulation was detected in sheep lung tissue exposed to FE fibers, suggesting that apoptosis is an important mechanism used to remove cells with FE-induced genetic changes, which predispose the involved tissue to neoplastic development (Loreto et al., 2008). The overexpression of the phosphorylated retinoblastoma protein (pRb) in alveolar epithelium and interstitium, close to the FE fibers, has also been detected (Musumeci et al., 2010). These data suggest that the pRb up-regulation could be a programmed response of cells to protect the organism against their uncontrolled proliferation. Since there is a close link between chronic inflammation and cancer development (Balkwill and Mantovani, 2001) and there are different findings confirming inflammatory pathophysiology of FE fibers in lung tissue, our actual interest is to investigate the involvement of N-Cad, AQP1 and ADAM-10 in the pathophysiology related to the exposure to FE fibers. N-Cad is a transmembrane glycoprotein that mediates cell-cell adhesion and plays an important role in the embryonic development and maintenance of normal adult tissue architecture (Nollet et al., 2000). It is useful in determining the histogenetic origin of tumors because of its altered expression in carcinogenesis (Nelson and Ordonez, 2003). Tan and coauthors demonstrated, in most bladder cancer tissues, an increased N-Cad and fibronectin expression and a decreased E-cadherin expression, suggesting an EMT that represents the initial stage of tumor progression (Tan et al., 2014). Moreover, the N-cadherin overexpression in cancer stimulates migration and invasion of cells (Derycke and Bracke, 2004). N-cadherin has also been indicated as an angiogenic factor in non small-cell lung cancer as biopsies positive for N-cadherin were hypervascular (Nakashima et al., 2003). Our results, both densitometric and morphometric analysis, showed an overexpression of N-Cad in lung tissue of FE exposed sheep, and although the N-Cad has multiple functions, we consider it interesting to analyze the data as a possible witness of the carcinogenic process. The overexpression of ADAM-10 has been reported for various types of cancer (Murphy, 2008) suggesting its direct role in cell signalling during the tumor progression (Saftig and Reiss, 2011). The release of cell adhesion molecules including L1, L-selectin, CD44, E-cadherin and N-cadherin affects cell-cell interaction and cell migration as well as cell signalling (Saftig and Reiss, 2011). ADAM-10 can also induce N-cadherin cleavage (Reiss et al., 2005) resulting in changes in the adhesive behavior of cells and also in a redistribution of β-catenin from the cell surface to the cytoplasmic pool, influencing the expression of β-catenin target genes (Saftig and Reiss, 2011) and finally promoting cancer pathogenesis. Additionally, ADAM-10 could be involved in tumors that are dependent on EGFR/Her-2 signalling (Saftig and Reiss, 2011). ADAM-10 mediates the constitutive release of TNF-α and IL-6R (Matthews et al., 2003; Hikita et al., 2009), and modulates the function of cell adhesion molecules involved in the process of leukocyte recruitment during inflammation (Saftig and Reiss, 2011). ADAM-10 could be critically involved in the shedding of Fas ligand (FasL) (Schulte et al., 2007) involved in the downregulation of immune reactions by activation of apoptosis, observed in our previous studies (Musumeci et al., 2014c). ADAM-10 also regulates endothelial permeability and T-cell transmigration by

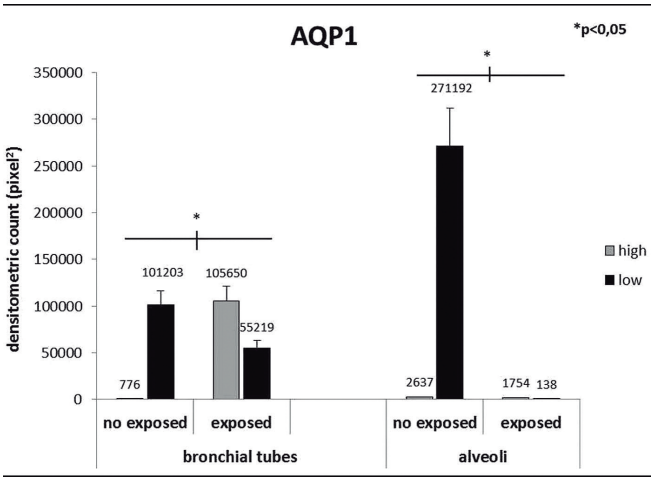

Fig. 10. Graph. A bar chart representing a comparison of the immunostaining intensity in AQP1 positive areas of non exposed sheep (n. 10) vs. exposed sheep (n. 60), expressed by densitometric count (pixel2) of dark brown pixels of the analyzed fields. Gray bars, high immunostaining; black bars, low immunostaining. Data are presented as mean±SD. *p<0,05.

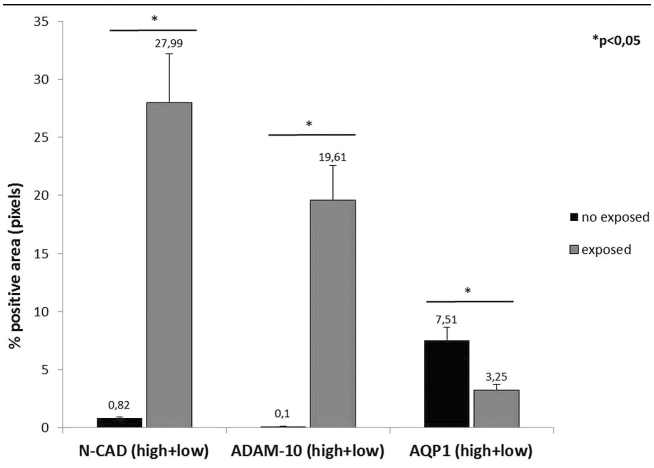

Fig. 11. Graph. A bar chart representing a comparison of the % N-cad, ADAM-10 and AQP1 immunostained area in non exposed sheep (n. 10) vs. exposed sheep (n. 60), expressed by % positive, dark brown pixels of the analyzed fields. Data are presented as mean±SD. *p<0,05.

shedding of vascular endothelial VE-cadherin (Schulz et al., 2008). Our previous studies on effects of FE fiber exposure on lung tissue support the inflammatory nature of the pathological process, and the results of the present study further confirm this mechanism. In fact, our results, both densitometric and morphometric analysis, showed an overexpression of ADAM-10 in lung tissue of FE exposed sheep. In relation to AQP1, our study on its expression in lung tissue of FE exposed sheep had a completely different meaning, which is not related to its possible negative effects, but rather to its regulatory role in tissue homeostasis. AQP1 is physiologically expressed in normal tissues, suggesting that it has an important regulatory role for cell volume and extracellular matrix homeostasis (Richardson et al., 2008; Loreto et al., 2012; Musumeci, 2013). The overexpression of AQP1 suggests that it may play a role in edema by interfering with water-reserve mechanisms and water balance disorders. AQP1 activation, induced by pathological processes, may be an endogenous mechanism used to control tissue degeneration (Musumeci, 2013). Moreover, Jablonski and coauthors, demonstrated that in cell culture, AQP-mediated water permeability of cell membrane can control the rate of apoptosis, demonstrating a strict correlation between overexpression of AQP1 and apoptosis (Jablonski et al., 2004). Our results in densitometric and morphometric analysis showed a complex pattern in AQP1 expression. In fact, in control sheep lung, an extensive but low AQP1 immunostaining was detected everywhere in lung tissue, testifying its regulatory role in cell and extracellular matrix homeostasis. On the contrary, in exposed sheep lung, we detected an overexpression of AQP1 in fibrotic interstitium around bronchial tubes and in some areas of bronchial epithelium, testifying its probable role in a cellular response to FE fibers, which could be explained by its attempt to regulate tissue homeostasis in some altered condition such as fibrosis (Martinez et al., 2006; Loreto et al., 2008). Interestingly, we showed no AQP1 expression in interstitium between alveoli and in alveolar epithelium, probably causing, in the advanced stage of the lesions, the destruction of lung architecture with irregular enlargement of the alveolar cavities and consequent honeycombing, as we showed in our previous histological studies (Martinez et al., 2006; Loreto et al., 2008). Moreover, from morphometric analysis, although distribution and intensity of AQP1 immunolabeling showed a more complex pattern as reported above, the total percentage of immunostained areas by AQP1 was higher in non exposed sheep compared to exposed ones.

Conclusion

In conclusion, the results of this study support the possible involvement of N-Cad, ADAM-10 and AQP1 in pathological processes induced by FE fiber exposure in lung tissue, even if with distinct roles. N-Cad could be involved in the onset of cancer, such as the pleural mesothelioma. ADAM-10 is involved in both the inflammatory processes and in the eventual onset of carcinogenesis. AQP1, instead, seems to be involved in the endogenous regulatory mechanisms activated by FE fiber exposure, in order to restore tissue homeostasis. The association between FE fiber exposure and the expression of N-Cad, ADAM-10 and AQP1 could be a topic for further studies, in order to find a treatment for the population exposed.

Acknowledgements. This study was supported by grants provided by FIR 2014-2016, University of Catania, Italy. The authors would like to thank Prof. Iain Halliday for commenting and making corrections to the paper.

Conflict of Interest. The authors have no conflict of interest.

References

Abutaily A.S., Collins J.E. and Roche W.R. (2003). Cadherins, catenins and APC in pleural malignant mesothelioma. J. Pathol. 201, 355-362.

Balkwill F. and Mantovani A. (2001). Inflammation and cancer: back to Virchow? Lancet 357, 539-545.

Begin R., Rola-Pleszczynski M., Sirois P., Masse S., Nadeau D. and Bureau M.A. (1981). Sequential analysis of the bronchoalveolar milieu in conscious sheep. J. Appl. Physiol. 50, 665-671.

Biggeri A., Pasetto R., Belli S., Bruno C., Di Maria G., Mastrantonio M., Trinca S., Uccelli R. and Comba P. (2004). Mortality from chronic obstructive pulmonary disease and pleural mesothelioma in an area contaminated by natural fiber (fluoro-edenite). Scand. J. Work. Environ. Health. 30, 249-252.

Cai J., Guan H., Fang L., Yang Y., Zhu X., Yuan J., Wu J. and Li M. (2013). MicroRNA-374a activates Wnt/beta-catenin signalling to promote breast cancer metastasis. J. Clin. Invest. 123, 566-579.

Cardile V., Lombardo L., Belluso E., Panico A., Renis M., Gianfagna A. and Balazy M. (2007). Fluoro-edenite fibers induce expression of Hsp70 and inflammatory response. Int. J. Environ. Res. Public. Health. 4, 195-202.

Comba P., Gianfagna A. and Paoletti L. (2003). Pleural mesothelioma cases in Biancavilla are related to a new fluoro-edenite fibrous amphibole. Arch. Environ. Health 58, 229-232.

Derycke L.D. and Bracke M.E. (2004). N-cadherin in the spotlight of cell-cell adhesion, differentiation, embryogenesis, invasion and signalling. Int. J. Dev. Biol. 48, 463-476.

Fogel M., Gutwein P., Mechtersheimer S., Riedle S., Stoeck A., Smirnov A., Edler L., Ben-Arie A., Huszar M. and Altevogt P. (2003). L1 expression as a predictor of progression and survival in patients with uterine and ovarian carcinomas. Lancet 362, 869-875.

Gavert N., Conacci-Sorrell M., Gast D., Schneider A., Altevogt P., Brabletz T. and Ben-Ze'ev A. (2005). L1, a novel target of beta-catenin signalling, transforms cells and is expressed at the invasive front of colon cancers. J. Cell Biol. 168, 633-642.

Gianfagna A. and Oberti R. (2001). Fluoro-edenite from Biancavilla (Catania, Sicily, Italy): crystal chemistry of a new amphibole end-member. Am. Mineralog. 86, 1489-1493.

Hatta K., Takagi S., Fujisawa H. and Takeichi M. (1987). Spatial and temporal expression pattern of N-cadherin cell adhesion molecules correlated with morphogenetic processes of chicken embryos. Dev.

Biol. 120, 215-227.

Hikita A., Tanaka N., Yamane S., Ikeda Y., Furukawa H., Tohma S., Suzuki R., Tanaka S., Mitomi H. and Fukui N. (2009). Involvement of A Disintegrin And Metalloproteinase 10 and 17 in shedding of tumor necrosis factor-alpha. Biochem. Cell. Biol. 87, 581-593.

Hundhausen C., Schulte A., Schulz B., Andrzejewski M.G., Schwarz N., von Hundelshausen P., Winter U., Paliga K., Reiss K., Saftig P., Weber C. and Ludwig A. (2007). Regulated shedding of transmembrane chemokines by the disintegrin and metalloproteinase 10 facilitates detachment of adherent leukocytes. J. Immunol. 178, 8064-8072.

Jablonski E.M., Webb A.N., McConnell N.A., Riley M.C. and Hughes F.M. Jr (2004). Plasma membrane aquaporin activity can affect the rate of apoptosis but is inhibited after apoptotic volume decrease. Am. J. Physiol. Cell. Physiol. 286, 975-985.

Kamp D.W. and Weitzman S.A. (1999). The molecular basis of asbestos induced lung injury. Thorax 54, 638-652.

Kamp D.W., Graceffa P., Pryor A. and Wetzman S.A. (1992). The role of free radicals in asbestos-induced diseases. Free Radic. Biol. Med. 12, 293-315.

Kim M.C., Cui F.J. and Kim Y. (2013). Hydrogen peroxide promotes epithelial to mesenchymal transition and stemness in human malignant mesothelioma cells. Asian Pac. J. Cancer. Prev. 14, 3625-3630.

King J.E., Thatcher N., Pickering C.A.C. and Hasleton P.S. (2006). Sensitivity and specificity of immunohistochemical markers used in the diagnosis of epithelioid mesothelioma: a detailed systematic analysis using published data. Histopathology 48, 223-232.

Lee T.C., Gold L., Aston J.R.C., Begin R. and Jaishree Jagirdar W.N.R. (1997). Immunohistochemical localization of transforming growth factor-ß and insulin-like growth factor-I in asbestosis in the sheep model. Int. Arch. Occup. Environ. Health 69, 157-164.

Liang H.T., Feng X.C. and Ma T.H. (2008). Water channel activity of plasma membrane affects chondrocyte migration and adhesion. Clin. Exp. Pharmacol. Physiol. 35, 7-10.

Loreto C., Rapisarda V., Carnazza M.L., Musumeci G., Valentino M., Fenga C. and Martinez G. (2008). Fluoro-edenite fibres induce lung cell apoptosis: an in vivo study. Histol. Histopathol. 23, 319-326.

Loreto C., Carnazza M.L., Cardile V., Libra M., Lombardo L., Malaponte G., Martinez G., Musumeci G., Papa V. and Cocco L. (2009). Mineral fibers-mediated activation of phosphoinositide-specific phospholipase c in human bronchoalveolar carcinoma-derived alveolar epithelial a549 cells. Int. J. Oncol. 34, 371-376.

Loreto C., Lo Castro E., Musumeci G., Loreto F., Rapisarda G., Rezzani R., Castorina S., Leonardi R. and Rusu M.C. (2012). Aquaporin 1 expression in human temporomandibular disc. Acta. Histochem. 114, 744-748.

Loreto C., Leonardi R., Musumeci G., Pannone G. and Castorina S. (2013). An ex vivo study on immunohistochemical localization of MMP-7 and MMP-9 in temporomandibular joint discs with internal derangement. Eur. J. Histochem. 57, e12.

Martinez G., Loreto C., Rapisarda V., Masumeci G., Valentino M. and Carnazza M.L. (2006). Effects of exposure to fluoro-edenite fibre pollution on the respiratory system: an in vivo model. Histol. Histopathol. 21, 595-601.

Matthews V., Schuster B., Schutze S., Bussmeyer I., Ludwig A., Hundhausen C., Sadowski T., Saftig P., Hartmann D., Kallen K.J. and Rose-John S. (2003). Cellular cholesterol depletion triggers shedding of the human interleukin-6 receptor by ADAM10 and ADAM17 (TACE). J. Biol. Chem. 278, 38829-38839.

McCulloch D.R., Akl P., Samaratunga H., Herington A.C. and Odorico D.M. (2004). Expression of the disintegrin metalloprotease, ADAM-10, in prostate cancer and its regulation by dihydrotestosterone, insulin-like growth factor I, and epidermal growth factor in the prostate cancer cell model LNCaP. Clin. Cancer Res. 10, 314-323.

Mobasheri A. and Marples D. (2004). Expression of the AQP-1 water channel in normal human tissues: a semiquantitative study using tissue microarray technology. Am. J. Physiol. Cell. Physiol. 286, 529-537.

Murphy G. (2008). The ADAMs: signalling scissors in the tumour microenvironment. Nat. Rev. Cancer 8, 929-941.

Musumeci G. (2013). The role of AQP1 in knee osteoarthritis (OA): A contemporary review. OA. Arthritis. 1, 1-6.

Musumeci G., Loreto C., Cardile V., Carnazza M.L. and Martinez G. (2010). Immunohistochemical expression of retinoblastoma and phospho-retinoblastoma protein in sheep lung exposed to fluoro-edenite fibers. Anat. Sci. Int. 85, 74-78.

Musumeci G., Cardile V., Fenga C., Caggia S. and Loreto C. (2011). Mineral fibre toxicity: expression of retinoblastoma (Rb) and phospho-retinoblastoma (pRb) protein in alveolar epithelial and mesothelial cell lines exposed to fluoro-edenite fibres. Cell. Biol. Toxicol. 27, 217-225.

Musumeci G., Leonardi R., Carnazza M.L., Cardile V., Pichler K., Weinberg A.M. and Loreto C. (2013a). Aquaporin 1 (AQP1) expression in experimentally induced osteoarthritic knee menisci: an in vivo and in vitro study. Tissue Cell 45, 145-152.

Musumeci G., Castrogiovanni P., Loreto C., Castorina S., Pichler K. and Weinberg A.M. (2013b). Post-traumatic caspase-3 expression in the adjacent areas of growth plate injury site: a morphological study. Int. J. Mol. Sci. 14, 15767-15784.

Musumeci G., Trovato F.M., Pichler K., Weinberg A.M., Loreto C. and Castrogiovanni P. (2013c). Extra-virgin olive oil diet and mild physical activity prevent cartilage degeneration in an osteoarthritis model. An "in vivo" and "in vitro" study on lubricin expression. J. Nutr. Biochem. 24, 2064-2075.

Musumeci G., Loreto C., Leonardi R., Castorina S., Giunta S., Carnazza M.L., Trovato F.M., Pichler K. and Weinberg AM. (2013d). The effects of physical activity on apoptosis and lubricin expression in articular cartilage in rats with glucocorticoid-induced osteoporosis. J. Bone. Miner. Metab. 31, 274-284.

Musumeci G., Imbesi R., Magro G., Parenti R., Szychlinska M.A., Scuderi R., Castorina S. and Castrogiovanni P. (2014a). N-cadherin has a protective role in stable human atherosclerotic plaques: a morphological and immunohistochemical study. J. Histol. Histopathol. 1:4.

Musumeci G., Trovato F.M., Imbesi R. and Castrogiovanni P. (2014b) Effects of dietary extra-virgin olive oil on oxidative stress resulting from exhaustive exercise in rat skeletal muscle: A morphological study. Acta Histochem. 116, 61-69.

Musumeci G., Coleman R., Imbesi R., Magro G., Parenti R., Szychlinska M.A., Scuderi R., Cinà C.S., Castorina S. and Castrogiovanni P. (2014c). ADAM-10 could mediate cleavage of N-cadherin promoting apoptosis in human atherosclerotic lesions leading to vulnerable plaque: A morphological and immunohistochemical study. Acta Histochem. 116, 1145-1158.

Nakashima T., Huang C., Liu D., Kameyama K., Masuya D., Kobayashi S., Kinoshita M. and Yokomise H. (2003). Neural-cadherin expression associated with angiogenesis in non-small-cell lung

cancer patients. Br. J. Cancer 88, 1727-1733.

Nelson G. and Ordonez M.D. (2003). Value of E-Cadherin and N-Cadherin immunostaining in the diagnosis of mesothelioma human pathology. Hum. Pathol. 34, 749-755.

Nollet F., Kools P. and van Roy F. (2000). Phylogenetic analysis of the cadherin superfamily allows identification of six major subfamilies besides several solitary members. J. Mol. Biol. 299, 551-572.

Paoletti L., Batisti D., Bruno C., Di Paola M., Gianfagna A., Mastrantonio M., Nesti M. and Comba P. (2000). Unusually high incidence of malignant pleural mesothelioma in a town of eastern Sicily: an epidemiological and environmental study. Arch. Environ. Health 55, 392-398.

Pugnaloni A., Lucarini G., Giantomassi F., Lombardo L., Capella S., Belluso E., Zizzi A., Panico A.M., Biagini G. and Cardile V. (2007). In vitro study of biofunctional indicators after exposure to asbestos-like fluoro-edenite fibres. Cell. Mol. Biol. (Noisy-le-grand). 53, 965-980.

Redies C., Engelhardt K. and Takeichi M. (1993). Differential expression of N- and R-cadherin in functional neuronal systems and other structures of the developing chicken brain. J. Comp. Neurol. 333, 398-416.

Reiss K., Maretzky T., Ludwig A., Tousseyn T., de Strooper B., Hartmann D. and Saftig P. (2005). ADAM10 cleavage of N-cadherin and regulation of cell–cell adhesion and beta-catenin nuclear signalling. EMBO J. 2, 742-752.

Reiss K. and Saftig P. (2009). The “A Disintegrin And Metalloprotease” (ADAM) family of sheddases: physiological and cellular functions. Semin. Cell. Dev. Biol. 20, 126-137.

Richardson S.M., Knowles R., Marples D., Hoyland J.A. and Mobasheri A. (2008). Aquaporin expression in the human intervertebral disc. J. Mol. Histol. 39, 303-309.

Rinaudo C., Cairo S., Gastaldi D., Gianfagna A., Mazziotti Tagliani S., Tosi G. and Conti C. (2006). Characterization of fluoro-edenite by m-Raman and m-FTIR spectroscopy. Mineralog. Mag. 70, 291-298.

Saftig P. and Reiss K. (2011). The “A Disintegrin And Metalloproteases” ADAM10 and ADAM17: Novel drug targets with therapeutic potential? Eur. J. Cell. Biol. 90, 527-535.

Schulte M., Reiss K., Lettau M., Maretzky T., Ludwig A., Hartmann D., de Strooper B., Janssen O. and Saftig P. (2007). ADAM10 regulates FasL cell surface expression and modulates FasL-induced cytotoxicity and activation-induced cell death. Cell Death Differ. 14, 1040-1049.

Schulz B., Pruessmeyer J., Maretzky T., Ludwig A., Blobel C.P., Saftig P. and Reiss K. (2008). ADAM10 regulates endothelial permeability and T-Cell transmigration by proteolysis of vascular endothelial cadherin. Circ. Res. 102, 1192-1201.

Sindelar B.J., Evanko S.P., Alonzo T., Herring S.W. and Wight T. (2000). Effects of intraoral splint wear on proteoglycans in the temporomandibular joint disc. Arch. Biochem. Biophys. 379, 64-70.

Soler A.P. and Knudsen K.A. (1994). N-cadherin involvement in cardiac myocyte interaction and myofibrillogenesis. Dev. Biol. 162, 9-17.

Szychlinska M.A., Parenti R., Loreto C., Salvatorelli L., Spadola S., Trovato F.M., Pirri C., Rapisarda V., Pace M.M., Magro G. and Musumeci G. (2014). Fluoro Edenite-associated pathogenesis in Pleural Malignant Mesothelioma. Acta Medica Mediterranea 30, 981-989.

Tan M., Gong H., Zeng Y., Tao L., Wang J., Jiang J., Xu D., Bao E., Qiu J. and Liu Z. (2014). Downregulation of Homeodomain-Interacting Protein Kinase-2 Contributes to Bladder Cancer Metastasis by Regulating Wnt Signalling. J. Cell. Biochem. 115, 1762-1767.

Tousseyn T., Jorissen E., Reiss K. and Hartmann D. (2006). (Make) stick and cut loose-disintegrin metalloproteases in development and disease. Birth Defects Res. C. Embryo. Today 78, 24-46.

Verkman A.S. (2009). Knock-out models reveal new aquaporin functions. Handb. Exp. Pharmacol. 190, 359-381.

Wang F. and Zhu Y. (2011). Aquaporin-1: a potential membrane channel for facilitating the adaptability of rabbit nucleus pulposus cells to an extracellular matrix environment. J. Orthop. Sci. 16, 304-312.

Wu E., Croucher P.I. and McKie N. (1997). Expression of members of the novel membrane linked metalloproteinase family ADAM in cells derived from a range of haematological malignancies. Biochem. Biophys. Res. Commun. 235, 437-442.

Yoshimura T., Tomita T., Dixon M.F., Axon A.T., Robinson P.A. and Crabtree J.E. (2002). ADAMs (A Disintegrin And Metalloproteinase) messenger RNA expression in Helicobacter pylori-infected, normal, and neoplastic gastric mucosa. J. Infect. Dis. 185, 332-340.

Accepted March 10, 2015